




A Narrowband Optical Perfect Absorber and Refractive Index Sensor Based on an Epsilon-Near-Zero Metamaterial Using Ag-Ge-Si Nanowires

Behnoush Ghafari¹ · Mohammad Danaie¹  · Majid Afsahi¹

Received: 17 June 2023 / Accepted: 11 October 2023 / Published online: 22 October 2023
© The Author(s) under exclusive licence to Sociedade Brasileira de Física 2023

Abstract

In this paper, a narrowband optical absorber with an absorption peak of 99.9% at the telecommunication wavelength of 1310 nm is presented. It consists of nanowires composed of five periods of Ag-Ge-Si disks on a Si substrate. The design of the stacks is based on epsilon-near-zero (ENZ) metamaterials, which causes this structure to have a relatively small thickness (i.e., thickness $< 5\lambda$, where λ is the working wavelength). By adjusting the thickness of the stacks using the effective medium theory (EMT) model, we have achieved the desired ENZ wavelength. The perfect absorption feature has been obtained by the synergy of resonances of surface plasmon polaritons (SPP) and ENZ modes. The proposed structure has been simulated using the finite difference frequency domain method. The simulation results indicate that the absorption rate remains almost 90% up to an angle of 75° and is insensitive to polarization. Furthermore, by changing the arrangement of the neighboring stacks, we see an increase in the sensitivity of the absorption peak to the refractive index variations of the environment. In general, narrowband absorbers have good potentials for applications such as filtering, sensing, and detecting, which underlines the significance of this work.

Keywords Narrowband absorber · Epsilon-near-zero · Nanowire · Effective medium theory · Metamaterial

1 Introduction

Due to the diverse and extensive application of electromagnetic (EM) wave absorbers, including filters, thermal emitters, and biosensors, special attention is paid to the study and investigation of these structures [1–6]. These absorbers are also widely used as highly sensitive refractive index sensors [7–12]. The two leading challenges in the design of absorbers are the use of materials with high optical losses and high thickness. With the advent of plasmonic materials and metamaterials made, it has become possible to design absorbers with sub-wavelength thicknesses [13]. In recent years, a huge amount of research has been conducted on epsilon-near-zero (ENZ) metamaterials, which

shows the unique characteristics of these materials [14]. Albeit it should be noted that ENZ materials are not naturally found in nature and to engineer the ENZ wavelength for the desired range, metamaterial structures can be used [15, 16]. Metamaterial science is the science of engineering materials to achieve unique and unorthodox electrical and magnetic properties. By modifying and adjusting the electric permittivity and magnetic permeability, which are significant factors in the interaction between light and matter, new optical devices with unique characteristics can be created [17–19]. There are generally two methods for achieving this goal: isotropic epsilon-near-zero (IENZ) and anisotropic epsilon-near-zero (AENZ) approaches. In the IENZ approach, the plasma frequency (ω_p) can be altered using chemical methods and impurities in metal-dielectric compounds, resulting in the formation of isotropic ENZ structures. In the AENZ method, either a layered structure (uniaxial) or an array of metal nanorods in a dielectric environment (two-dimensional) can be employed [20, 21]. One of the simplest methods to achieve the ENZ mode at the desired wavelength is to use alternating layered metamaterial structures consisting of metal, dielectric, and semiconductor stacks [16, 22–25]. Due to the sub-wavelength thickness of

✉ Mohammad Danaie
danaie@semnan.ac.ir

Behnoush Ghafari
ghafari.behnoosh@semnan.ac.ir

Majid Afsahi
m_afsahi@semnan.ac.ir

¹ Faulty of Electrical and Computer Engineering, Semnan University, Semnan, Iran

the stacks, equivalent optical properties of the structure can be achieved by using the effective medium model, which is a homogenization method based on field averaging [26]. By investigating and relying on the characteristics of ENZ materials such as strong light-matter interactions, nanoscale field confinement, and enhancement [27], we can move towards improving and overcoming the challenges of achieving complete absorption.

In [28], an ultra-small-sized and ultra-broadband absorber based on an array of nanowires composed of metal-dielectric stacks is presented. Excitation of the gap surface plasmon polariton (G-SPP) mode in a Fabry–Perot (FP)-like resonator has caused broadband absorption in the wavelength range of 0.2 to 7 μm with an average absorption of 91%. In [29], a metal-dielectric multilayer nanoantenna has been investigated based on the hybrid modes from SPPs. One of the important advantages of multilayer structures is the possibility of easy experimental fabrication. A broadband absorber based on a core–shell nanowire model is presented in [30]. In this structure, silicon is coated as a core with a thin shell of gold, which can be manufactured in the real world using nanosphere lithography (NSL) and atomic layer deposition (ALD) techniques without any complex control process. The structure supports the multiple absorption peaks caused by the excitation of longitudinal and transverse surface plasmon modes under the irradiation of oblique incident waves with transverse electric (TE) and transverse magnetic (TM) polarization in the wavelength range of 400 to 1600 nm. The absorber presented in [31] consists of an array of gold nanowires in an aluminum host environment. For the absorber presented in [32], an almost complete absorption peak at the frequency of 195.9 THz occurs due to the cavity resonance mode.

In [4], an ultra-broadband omnidirectional absorber consisting of a stack of different semiconductors on a metal mirror is shown. The structure has an average absorption of 98% in a wide range of wavelengths from 400 to 2000 nm. The feature of ultra-broadband absorption is obtained in the structure of 5 tandem layers ($\text{MgF}_2\text{-TiO}_2\text{-Si-Ge-Cr}$) of three absorbing materials with resonances that overlap strongly [33]. In [34], the dielectric properties of various metal nanorods such as tungsten, gold, platinum, and titanium in the dielectric medium have been investigated using Maxwell Garnett's effective medium theory. The results indicate that the desired dielectric properties are affected by the appropriate selection of the type of metal and the dimensions of the metal rods.

In this article, we have tried to achieve a perfect absorber with a small thickness by using the field-confinement property of epsilon-near-zero metamaterials. In this regard, relying on the effective medium theory (EMT) model, nanowires consisting of metal–semiconductor-dielectric stacks with five periods have been placed on a metal substrate.

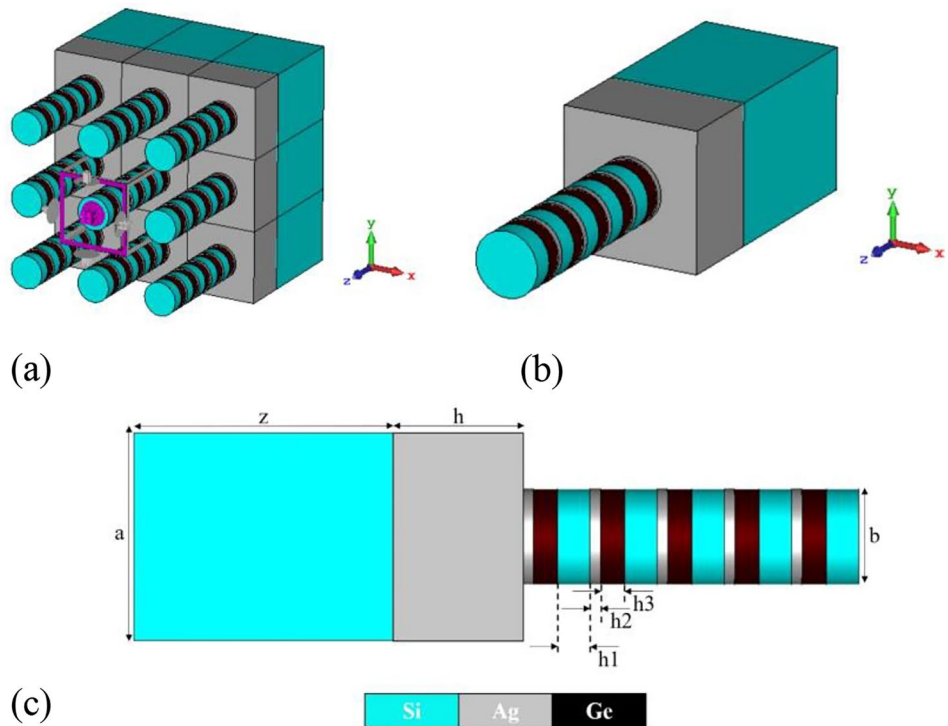
The thickness of the stacks is adjusted so that the effective permittivity of the structure at the telecommunication wavelength of 1310 nm is equal to zero. Then, by tuning the radius of the ENZ multilayer nanowires, the surface plasmon polariton (SPP) mode causes perfect absorption at the mentioned wavelength. The absorption peak is insensitive to polarization and remains more than 90% up to a 75° angle of incidence. This structure can also act as a refractive index sensor, which initially shows a modest sensitivity of 160 nm/refractive index unit (RIU), but by changing the arrangement of the stacks of adjacent nanowires (so that the field distribution is expanded in a larger space), a better sensitivity of 200 nm/RIU is obtained. It should be noted that all the simulations were performed using the hexahedral mesh analysis method, based on the finite difference frequency domain method of the CST Microwave Studio software. The boundary conditions are selected as periodic in the x and y directions of the unit cell and “open add-space” for the vertical (z) direction of the simulation region. The incident electromagnetic waves are perpendicular to the z surface of the structure.

2 Structure's Design Method

Sub-wavelength alternating multilayer structures are recognized as one of the simplest methods to achieve ENZ behavior. For this purpose, the metal-dielectric structure is commonly used [35, 36], but the metal–semiconductor-dielectric structures allow more control to adjust the ENZ wavelength in a wider range [37]. As shown in Fig. 1a, stacks of Ag metal, germanium, and silicon dielectric have been used to achieve epsilon-near-zero metamaterials at the telecommunication wavelength of 1310 nm. The mentioned wavelength is very important in optical communications due to its low attenuation, low dispersion, compatibility with existing infrastructure, avoidance of the water peak region, historical usage, standardization, and the availability of optical components optimized for this wavelength [38].

The Drude model describes the permittivity of silver as $\epsilon_{\text{Ag}}(\omega) = \epsilon_{\infty} - \frac{\omega_p^2}{\omega^2 - i\gamma\omega}$, where, $\epsilon_{\infty} = 5$, $\omega_p = 13.4 \times 10^{15}$ rad/s, and $\gamma = 0.7 \times 10^{14}$ rad/s. Here, ω_p is the plasma frequency of the bulk media and ϵ_{∞} denotes the medium dielectric constant for the infinite frequency. The dielectric constants of Ge and Si are $\epsilon_{\text{Ge}} = 16.2$ and $\epsilon_{\text{Si}} = 11.9$. [39, 40]. Due to the small thickness of the stacks in comparison with the desired working wavelength (which is as follows: $h_{\text{Ag}} = 8$ nm, $h_{\text{Ge}} = 19$ nm, and $h_{\text{Si}} = 25$ nm), the effective medium theory (EMT) can be used to set the ENZ wavelength. The effective permittivity of the proposed structure is obtained according to the following formula.

Fig. 1 **a** The 3D schematic of the proposed perfect absorber based on Ag-Ge-Si stacks. **b** Perfect absorber’s unit cell 3D view. **c** Perfect absorber 2D view (unit cell)



$$\epsilon_{eff} = \epsilon_0 \begin{pmatrix} \epsilon_{\parallel} & 0 & 0 \\ 0 & \epsilon_{\parallel} & 0 \\ 0 & 0 & \epsilon_{\perp} \end{pmatrix} \tag{1}$$

where the parameters ϵ_{\perp} and ϵ_{\parallel} represent the perpendicular and parallel components to the x - y plane, respectively. They are defined as:

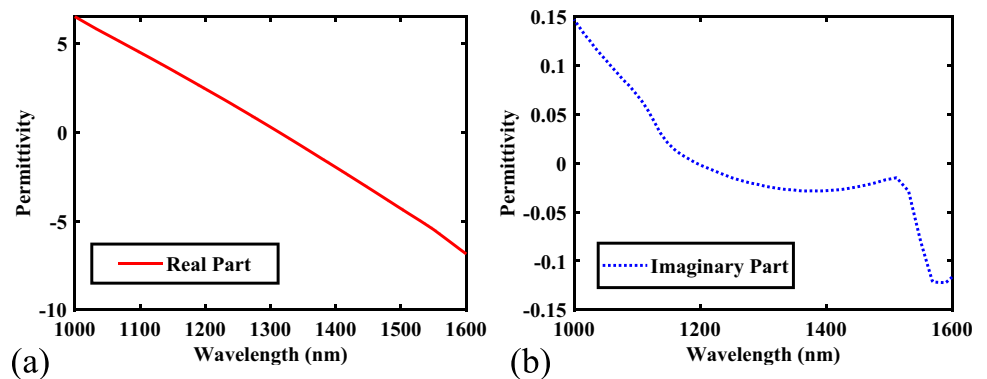
$$\epsilon_{\parallel} = \sum_j^{N_c} f_j \epsilon_j, j = 1, 2, 3 \tag{2}$$

$$\frac{1}{\epsilon_{\perp}} = \sum_j^{N_c} f_j \frac{1}{\epsilon_j}, j = 1, 2, 3 \tag{3}$$

f_j is the filling fractions and ϵ_j is the permeability of the j -layer. With the tuning of the thickness of the stacks, the value of ϵ_{\parallel} at the wavelength of 1310 nm is equal to zero. As a result, ϵ_{eff} also becomes zero at this wavelength (according to Fig. 2 and Eq. (1)) [41].

The proposed unit cell (according to Fig. 1b, c) consists of an ENZ nanowire with five alternations of Ag-Ge-Si stacks on an Ag metal and Si substrate with dimensions of 160 nm by 160 nm. By examining similar cases, it is estimated that if the total number of layers is considered to be at least 8 layers, it can be ensured that the structure is homogeneous [42]. In other words, a nanowire with an epsilon near zero is considered in an environment with an epsilon of 1. Based on the EMT model in the nanowire structure, ϵ_{\parallel} and ϵ_{\perp} can be calculated as [42]:

Fig. 2 The **a** real and **b** imaginary part of ϵ_{\parallel}



$$\epsilon_{\parallel} = \frac{(1 + f)\epsilon_{ENZ}\epsilon_{Air} + (1 - f)\epsilon_{ENZ}^2}{(1 - f)\epsilon_{Air} + (1 + f)\epsilon_{ENZ}} \tag{4}$$

$$\epsilon_{\perp} = f\epsilon_{ENZ} + (1 - f)\epsilon_{Air} \tag{5}$$

Considering the volume filling ratio $f = \frac{\pi r^2}{w \times w}$, it can be claimed that the value of ϵ_{\parallel} is approximately zero and the value of ϵ_{\perp} is around 1 [43, 44]. The result is the possibility of electromagnetic absorption. ENZ absorption excitation relies on Brewster angle with TM polarization or coupling with other modes [45]. Therefore, by tuning the radius of the nanowire, we provide the possibility of stimulating SPP mode at the adjusted ENZ wavelength, so that the coupling of the ENZ and SPP modes causes the confinement of the optical and electric fields in the sub-wavelength stacks and the strong absorption peak. As shown in Fig. 3, an almost perfect absorption of 99.9% occurred at a wavelength of 1310 nm.

The proposed absorber can be fabricated using the Raith e-LiNE method, which is an electron beam (E-beam) lithography system at a nanoscale level [46]. Next, by examining the changes in parameters such as the radius of the nanowire and the thickness of the layers, the effects of possible fabrication error in the manufacturing can be examined. To investigate the effect of the nanowire radius variation on the absorption peak wavelength, this parameter is swept while the other parameters are considered constant. For the design of the absorber, the radius of the nanowire is considered to be 37 nm, and by changing the radius from 31 to 40 nm with steps of 1 nm, we can see an increase in the wavelength of the absorption peak, as shown in Fig. 4. It is observed that by changing the excitation wavelength of

the SPP mode from the ENZ wavelength, the percentage of absorption decreases greatly.

As shown in Fig. 5, there are two distinct approaches which involve altering the thickness of the layers in Si (Fig. 5a), Ag (Fig. 5b), and Ge (Fig. 5c). In Si and Ge, as the thickness increases, the wavelengths also increase, and vice versa. Conversely, in Ag (Fig. 5b), wavelengths shift towards shorter values as the thickness increases and vice versa. This phenomenon also applies to the adjustment of ENZ wavelengths.

3 Results and Discussions

Figure 6 shows the absorption spectra for TM and TE polarizations under different incident angles. The results indicate that the proposed absorber is insensitive to polarization and sensitive to the incident angle. Nevertheless, the absorption percentage remains above 90% until the angle of 60°. It becomes almost zero at the angle of 90°. Achieving a polarization-insensitive design is due to the symmetry of the proposed structure [47]. Considering that the incident EM wave occurs at arbitrary directions in practical applications, insensitivity to polarization and low absorption variations over a relatively wide incident angle can be considered advantages [48]. To clarify the absorption mechanism of the proposed absorber structure, the distributions of the electric field (E), magnetic field (H), and current density (J) for TE and TM polarizations are shown in Fig. 7a, b, respectively. Areas with maximum field distribution are marked in red and regions with minimum field distribution are marked in blue. The electric

Fig. 3 The normalized absorption (A) and reflection (R) for the proposed absorber

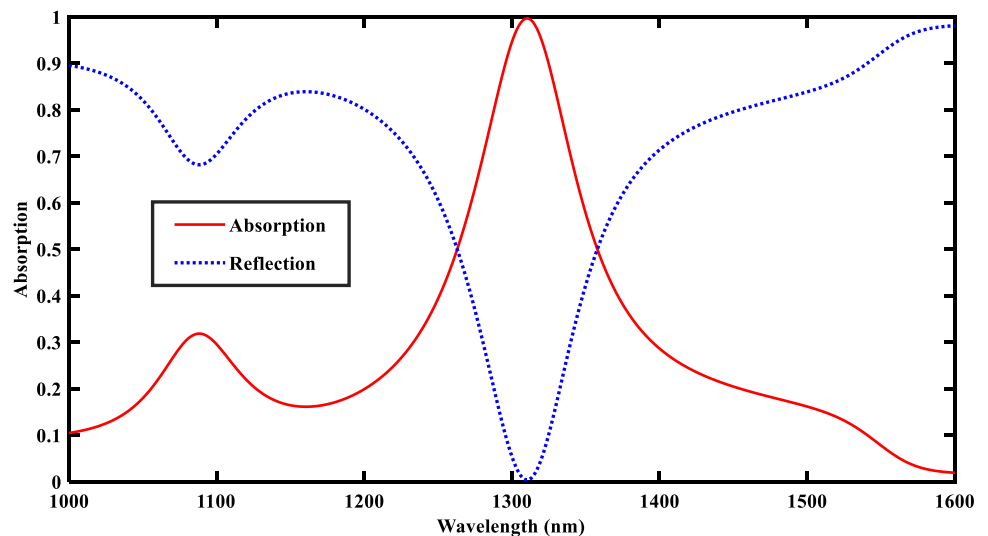
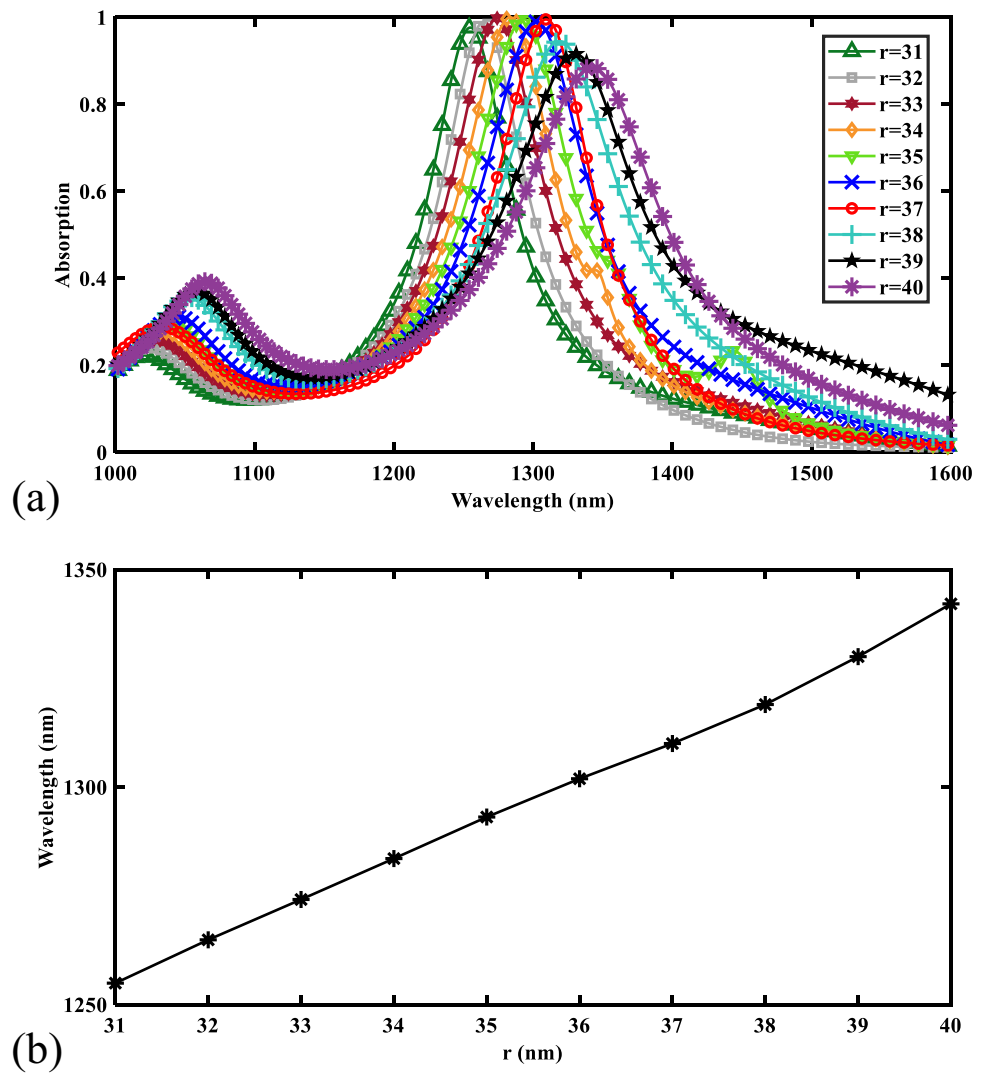


Fig. 4 The effect of nanowire radius on **a** absorption spectrum and **b** peak absorption wavelength



field distribution is mainly confined to the metal-dielectric and metal–semiconductor interface. Excitation of surface plasmon polaritons (SPP) at the metal interface causes strong absorption. The electric field is also confined in

the gap between two adjacent nanowires, which is of great importance.

Figure 8 shows the ratio of field distribution in different layers of the proposed structure. In our simulation,

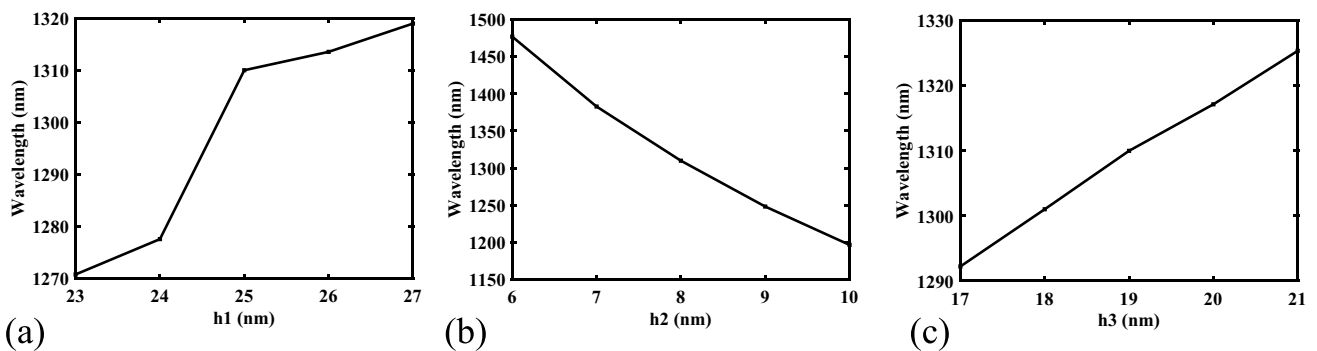


Fig. 5 The effect of thickness variation on peak absorption wavelength for **a** Si around $h_1=25$ nm, **b** Ag around $h_2=8$ nm, and **c** Ge around $h_3=19$ nm

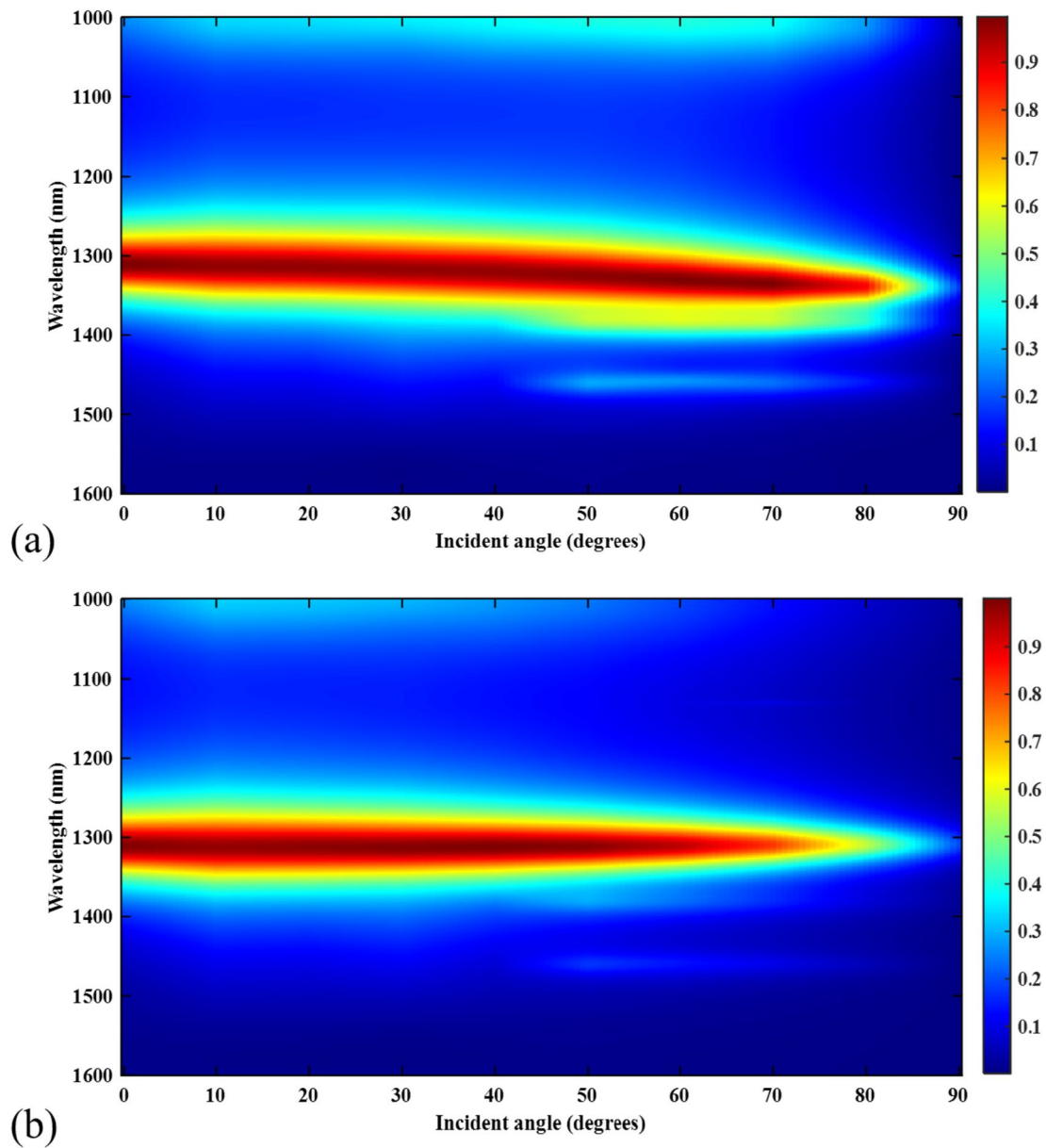


Fig. 6 Absorption spectra for different incident angles: **a** TE polarization and **b** TM polarization

the region from $z=-200$ nm to $z=0$ nm is considered the substrate, and that from $z=0$ nm to $z=100$ nm is the bottom layer of Ag. It is clear that the field distribution in these parts is zero. Meanwhile, the region from $z=100$ nm to $z=260$ nm is related to ENZ nanowire, where the field in its upper layers has the maximum value. The region from $z=360$ nm to $z=600$ nm is associated to the free space around the structure.

We have investigated the sensitivity of the proposed absorber to the refractive index of the medium for sensing

applications. By changing the refractive index of the medium as shown in Fig. 9a, the absorption peak is shifted to higher wavelengths. The sensitivity of the refractive index sensors is defined as

$$S = \frac{\Delta\lambda(\text{Peak})}{\Delta n} \left[\frac{\text{nm}}{\text{RIU}} \right] \tag{6}$$

where $\Delta\lambda$ stands for peaks wavelength shift and Δn is the refractive index variation. Hence, the sensitivity of this

Fig. 7 Distributions of E -field, H -field, and current density under **a** TE and **b** TM polarizations

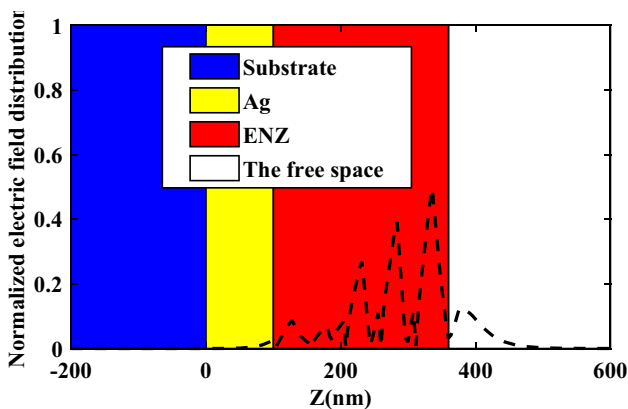
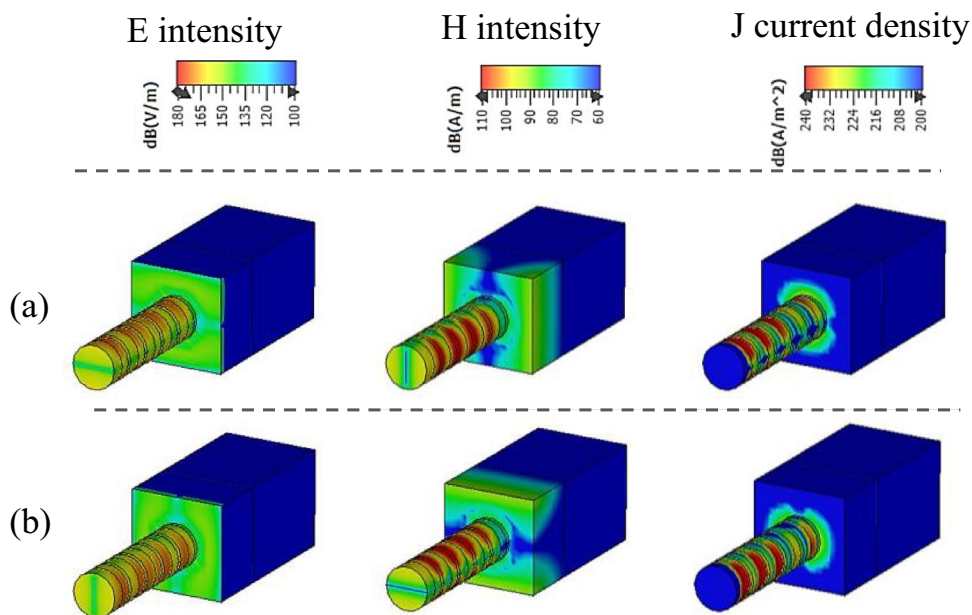


Fig. 8 Electric field magnitude distribution for the z direction of the structure

sensor is $160 \text{ nm}/\text{RIU}^{-1}$ [49]. To improve the sensory performance of this absorber, we reverse the arrangement of the stacks in the adjacent nanowires to increase the distribution of the electric field at the gap between two adjacent nanowires. As a result of this change, we can see an increase in the sensitivity of the sensor to the refractive index variations of the environment. According to Fig. 9b, the value of sensitivity is obtained as $S = 200$.

To better understand the issue, the two-dimensional distribution of the electric field between the gap of the adjacent nanowires in the y - z plane of the initial and improved design is shown in Fig. 10a and b, respectively [50]. The surface plasmons at the metal-dielectric boundaries can cause field confinement. Additionally, coupling occurs between adjacent nanowires, leading the electric field distribution

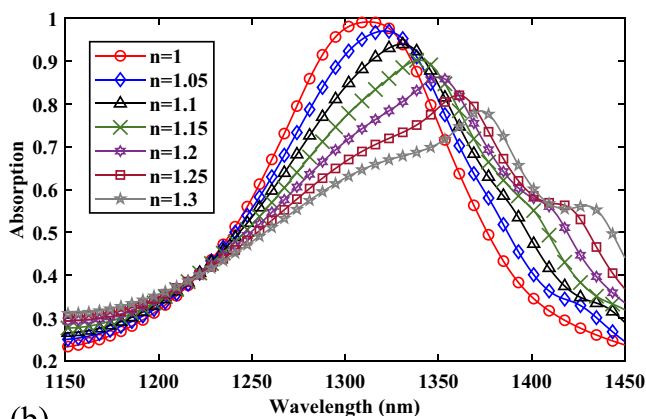
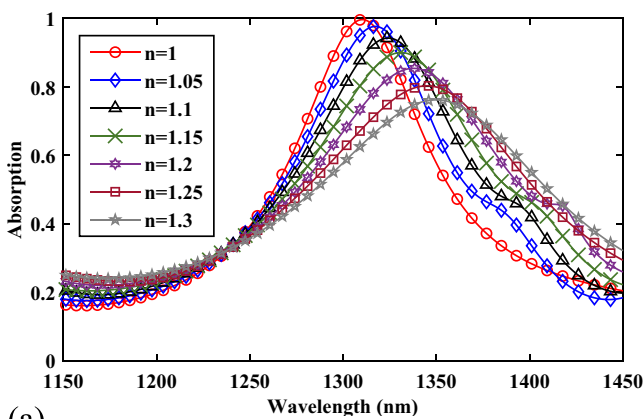


Fig. 9 A view of the absorption peak shift diagram in relation to the changes in the refractive index of the environment in **a** the initial design and **b** the improved design

Fig. 10 The distribution of the electric field in the gap between two adjacent nanowires in the y - z plane in **a** the initial design and **b** the improved design

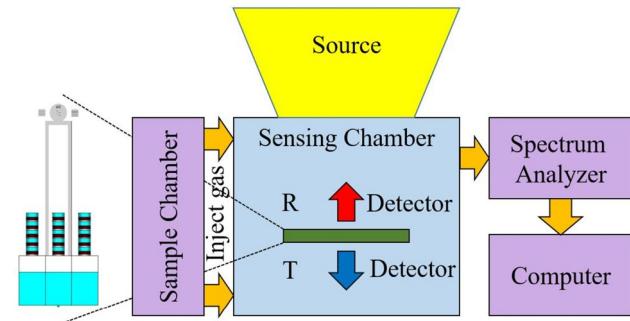
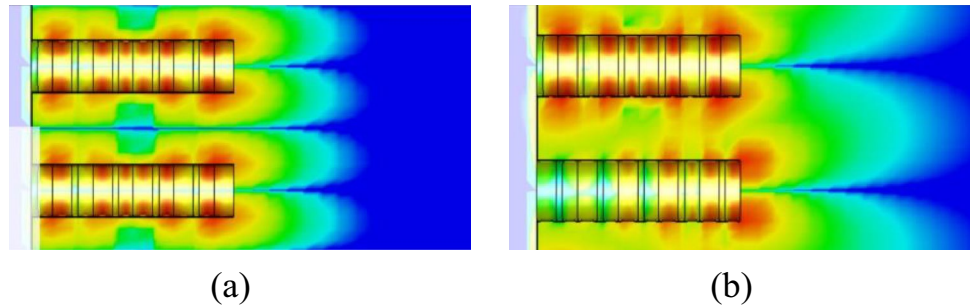


Fig. 11 Schematic of the sensor mechanism

to focus in the gap between nanowires, which enhances the interaction with the surrounding environment. In other words, it is crucial to confine the electric field distribution within the gap between the adjacent nanowires. By altering

the arrangement of the layers of the adjacent nanowires and by adjusting the position of the Ag metal layer, the field distribution in the gap can be increased, as illustrated in Fig. 10. Consequently, the sensitivity of the proposed sensor and its interaction with the environment are enhanced using the mentioned technique [51].

The proposed sensor operates as follows: the structure is placed inside a chamber, and the sample gas is injected into the structure (see Fig. 11). The electromagnetic waves are directed toward the structure, and by measuring the spectrum of the transmitted and reflected waves, the intensity and wavelength of absorption can be determined. By comparing these values with predetermined reference values, the refractive index of the sample gas is ascertained [52]. A comparison between some important parameters of the proposed perfect absorber and other works reported in the literature for this wavelength range is provided in Table 1.

Table 1 Comparison table of absorber parameters

Ref	Year	Absorption wavelengths (nm)	Absorption peaks (%)	Polarization sensitivity	Incident angle sensitivity
[30]	2013	1530	Perfect	Insensitive	Nearly omnidirectional
[53]	2021	1300	99.998	–	–
[54]	2023	874, 983, 1125	98.4, 97.2, 98.3,	–	–
[55]	2015	1536	95	–	–
[56]	2020	663	99.99	–	Insensitive
[57]	2019	488, 633, 941, 1864	About 99.37	–	–
[58]	2019	4071	99.2	Sensitive	Sensitive
[59]	2022	1490	99.99	Insensitive	Insensitive
[60]	2016	706	Perfect	Sensitive	–
This work	-	1310	99.9%	Insensitive	Wide incident angle insensitivity

4 Conclusions

In conclusion, we have introduced an absorber based on a novel epsilon-near-zero (ENZ) structure designed for the 1310 nm wavelength. The key advantage of this structure, along with the utilization of ENZ properties, is the achievement of perfect absorption with a thickness comparable to the operational wavelength (5λ). This perfect absorption feature results from the synergy between surface plasmon polariton (SPP) resonances and ENZ modes. The absorption ratio of the structure remains consistently high at approximately 90%, even up to an angle of 75° , and it is also insensitive to polarization. To enhance the sensitivity of the absorption peak to changes in the refractive index of the surrounding environment and improve its sensing capabilities, we have inverted the placement arrangement of the adjacent nanowire stacks. This modification widens the distribution of the electric field within the gap between the nanowires, resulting in an increased sensor sensitivity (S) from 160 to 200. Moreover, this innovative absorber has versatile applications beyond sensing, including its potential use as filters, emitters, and detectors.

Author Contribution Design, analysis, and investigation: BG; writing—original draft preparation: BG; writing, review, and editing: MD; supervision: MD and MA. We confirm that the manuscript has been read and approved by all named authors and that there are no other persons who satisfied the criteria for authorship but are not listed. We further confirm that the order of authors listed in the manuscript has been approved by all of us.

Data Availability The datasets generated and analyzed during the current study are available from the corresponding author on reasonable request.

Declarations

Ethical Approval Results are presented clearly, honestly, and without fabrication, falsification, or inappropriate data manipulation.

Conflict of Interest The authors declare no competing interests.

Consent to Participate Not applicable.

Consent for Publication Not applicable.

Disclaimer We the undersigned declare that the manuscript entitled “A narrowband optical perfect absorber and refractive index sensor based on an epsilon-near-zero metamaterial using Ag-Ge-Si nanowires” is original, has not been fully or partly published before, and is not currently being considered for publication elsewhere.

References

- M.R. Nickpay, M. Danaie, A. Shahzadi, Graphene-based metamaterial absorber for refractive index sensing applications in terahertz band. *Diam. Relat. Mater.* **130**, 109539 (2022)
- B. Ghafari, M. Danaie, M. Afsahi, Perfect absorber based on epsilon-near-zero metamaterial as a refractive index sensor. *Sens. Imaging* **24**(1), 15 (2023)
- M.R. Nickpay, M. Danaie, A. Shahzadi, A triple-band metamaterial graphene-based absorber using rotated split-ring resonators for THz biomedical sensing. *Opt. Quant. Electron.* **55**(2), 193 (2023)
- Y. Cui, Y. He, Y. Jin, F. Ding, L. Yang, Y. Ye, S. He, Plasmonic and metamaterial structures as electromagnetic absorbers. *Laser Photonics Rev.* **8**(4), 495–520 (2014)
- M.R. Nickpay, M. Danaie, A. Shahzadi, Graphene-based tunable quad-band fan-shaped split-ring metamaterial absorber and refractive index sensor for THz spectrum. *Micro Nanostruct.* **173**, 207473 (2023)
- L. Hajshahvaladi, H. Kaatuzian, M. Danaie, A high-sensitivity refractive index biosensor based on Si nanorings coupled to plasmonic nanohole arrays for glucose detection in water solution. *Opt. Commun.* **502**, 127421 (2022)
- M.R. Nickpay, M. Danaie, A. Shahzadi, A wideband and polarization-insensitive graphene-based metamaterial absorber. *Superlattices Microstruct.* **150**, 106786 (2021)
- M. Ghodrati, A. Mir, A. Farmani, 2D materials/heterostructures/metasurfaces in plasmonic sensing and biosensing. In *Plasmonics-Based Optical Sensors and Detectors* 339–371 (2024). Jenny Stanford Publishing
- M. Danaie, L. Hajshahvaladi, E. Ghaderpanah, A single-mode tunable plasmonic sensor based on an 8-shaped resonator for cancer cell detection. *Sci. Rep.* **13**(1), 13976 (2023)
- M.H. Sani, A. Ghanbari, H. Saghaei, High-sensitivity biosensor for simultaneous detection of cancer and diabetes using photonic crystal microstructure. *Opt. Quant. Electron.* **54**, 1–14 (2022)
- L. Hajshahvaladi, H. Kaatuzian, M. Moghaddasi, M. Danaie, Hybridization of surface plasmons and photonic crystal resonators for high-sensitivity and high-resolution sensing applications. *Sci. Rep.* **12**(1), 21292 (2022)
- M. Hosseinzadeh Sani, H. Saghaei, M.A. Mehranpour, A. Asgariyan Tabrizi, A novel all-optical sensor design based on a tunable resonant nanocavity in photonic crystal microstructure applicable in MEMS accelerometers. *Photonic Sens.* **11**, 457–471 (2021)
- A. Ghobadi, H. Hajian, B. Butun, E. Ozbay, Strong light–matter interaction in lithography-free planar metamaterial perfect absorbers. *ACS Photonics* **5**(11), 4203–4221 (2018)
- A. Anopchenko, L. Tao, H.W.H. Lee, Field-effect tunable epsilon-near-zero perfect absorbers. In *2017 Conference on Lasers and Electro-Optics Pacific Rim (CLEO-PR)* pp. 1–2 (2017, July). IEEE
- B. Johns, S. Chattopadhyay, J. Mitra, Tailoring infrared absorption and thermal emission with ultrathin film interferences in epsilon-near-zero media. *Adv. Photonics Res.* **3**(1), 2100153 (2022)
- J. Gao, L. Sun, H. Deng, C.J. Mathai, S. Gangopadhyay, X. Yang, Experimental realization of epsilon-near-zero metamaterial slabs with metal-dielectric multilayers. *Appl. Phys. Lett.* **103**(5), 051111 (2013)
- W.D. Newman, C.L. Cortes, J. Atkinson, S. Pramanik, R.G. DeCorby, Z. Jacob, Ferrell-Berremans modes in plasmonic epsilon-near-zero media. *ACS Photonics* **2**(1), 2–7 (2015)
- A. Ciallella, Research perspective on multiphysics and multiscale materials: a paradigmatic case. *Continuum Mech. Thermodyn.* **32**(3), 527–539 (2020)
- M.R. Nickpay, M. Danaie, A. Shahzadi, Design of a graphene-based multi-band metamaterial perfect absorber in THz frequency region for refractive index sensing. *Phys. E* **138**, 115114 (2022)
- P. Yu, L.V. Besteiro, J. Wu, Y. Huang, Y. Wang, A.O. Govorov, Z. Wang, Metamaterial perfect absorber with unabated size-independent absorption. *Opt. Express* **26**(16), 20471–20480 (2018)

21. N. Shankhwar, R.K. Sinha, Zero Index Metamaterials: Trends and Applications. Springer Nature. (2021)
22. D.S. Ginley, C. Bright, Transparent conducting oxides. *MRS bulletin* **25**(8), 15–18 (2000)
23. N. Shankhwar, R.K. Sinha, Zero Index Metamaterials: Trends and Applications. Springer Nature. (2021)
24. G. Subramania, A.J. Fischer, T.S. Luk, Optical properties of metal-dielectric based epsilon near zero metamaterials. *Appl. Phys. Lett.* **101**(24), 241107 (2012)
25. X. Yang, C. Hu, H. Deng, D. Rosenmann, D.A. Czaplewski, J. Gao, Experimental demonstration of near-infrared epsilon-near-zero multilayer metamaterial slabs. *Opt. Express* **21**(20), 23631–23639 (2013)
26. C. Cheng, Y. Lu, D. Zhang, F. Ruan, G. Li, Gain enhancement of terahertz patch antennas by coating epsilon-near-zero metamaterials. *Superlattices Microstruct.* **139**, 106390 (2020)
27. A.A. Orlov, P.M. Voroshilov, P.A. Belov, Y.S. Kivshar, Engineered optical nonlocality in nanostructured metamaterials. *Phys. Rev. B* **84**(4), 045424 (2011)
28. Z. Sakotic, A. Krasnok, N. Cselusyzka, N. Jankovic, A. Alú, Berreman embedded eigenstates for narrow-band absorption and thermal emission. *Phys. Rev. Appl.* **13**(6), 064073 (2020)
29. B. Wang, C. Ma, P. Yu, A.O. Govorov, H. Xu, W. Wang, Z. Wang, Ultra-broadband nanowire metamaterial absorber. *Photonics Res.* **10**(12), 2718–2727 (2022)
30. X.M. Zhang, J.J. Xiao, Q. Zhang, L.M. Li, Y. Yao, Plasmonic TM-like cavity modes and the hybridization in multilayer metal-dielectric nanoantenna. *Opt. Express* **23**(12), 16122–16132 (2015)
31. P. Buranasiri, S. Plaipichit, C. Puttharugsa, S. Wicharn, Hybrid nanowire-hyperbolic metamaterial based broadband absorber for the visible and near-infrared regions. *Radiat. Phys. Chem.* **189**, 109701 (2021)
32. Y. He, H. Deng, X. Jiao, S. He, J. Gao, X. Yang, Infrared perfect absorber based on nanowire metamaterial cavities. *Opt. Lett.* **38**(7), 1179–1181 (2013)
33. C. Yang, C. Ji, W. Shen, K.T. Lee, Y. Zhang, X. Liu, L.J. Guo, Compact multilayer film structures for ultrabroadband, omnidirectional, and efficient absorption. *ACS Photonics* **3**(4), 590–596 (2016)
34. L. Feng, P. Huo, Y. Liang, T. Xu, Photonic metamaterial absorbers: morphology engineering and interdisciplinary applications. *Adv. Mater.* **32**(27), 1903787 (2020)
35. M.A. Baqir, A. Farmani, M. Raza, M.N. Akhtar, A. Hussain, Engineering of metallic nanorod-based hyperbolic metamaterials for broadband applications operating in the infrared regime. *Appl. Nanosci.* **11**(1), 229–240 (2021)
36. A.R. Rashed, B.C. Yildiz, S.R. Ayyagari, H. Caglayan, Hot electron dynamics in ultrafast multilayer epsilon-near-zero metamaterials. *Phys. Rev. B* **101**(16), 165301 (2020)
37. S. Suresh, O. Reshef, M.Z. Alam, J. Upham, M. Karimi, R.W. Boyd, Enhanced nonlinear optical responses of layered epsilon-near-zero metamaterials at visible frequencies. *ACS Photonics* **8**(1), 125–129 (2020)
38. M. Vafaei, M. Moradi, G.H. Bordbar, Realization of epsilon-near-zero metamaterial stack based on dielectric-semiconductor-metal multilayers. *Plasmonics* **14**(6), 1929–1937 (2019)
39. X. Liu, K. Li, Z. Meng, Z. Zhang, Z. Wei, Hybrid metamaterials perfect absorber and sensitive sensor in optical communication band. *Front Phys* **9**, 125–129 (2021)
40. L. Hajshahvaladi, H. Kaatuzian, M. Danaie, Y. Karimi, Design of a highly sensitive tunable plasmonic refractive index sensor based on a ring-shaped nano-resonator. *Opt. Quantum Electron.* **54**(1), 1–17 (2022). <https://refractiveindex.info/>
41. T. Galfsky, Z. Sun, Z. Jacob, V.M. Menon, Preferential emission into epsilon-near-zero metamaterial. *Opt Mater Express* **5**(12), 2878–2883 (2015)
42. L. Ferrari, C. Wu, D. Lepage, X. Zhang, Z. Liu, Hyperbolic metamaterials and their applications. *Prog. Quantum Electron.* **40**, 1–40 (2015)
43. R. Starko-Bowes, J. Atkinson, W. Newman, H. Hu, T. Kallos, G. Palikaras, Z. Jacob, Optical characterization of epsilon-near-zero, epsilon-near-pole, and hyperbolic response in nanowire metamaterials. *JOSA B* **32**(10), 2074–2080 (2015)
44. V.B. Novikov, T.V. Murzina, Nonlocality-mediated spatiotemporal optical vortex generation in nanorod-based epsilon-near-zero metamaterials. *Opt. Lett.* **48**(8), 2134–2137 (2023)
45. I. Brener, F. Marquier, Theory of epsilon-near-zero modes in thin films (No. SAND2014–20631C). Sandia National Lab. (SNL-NM), Albuquerque, NM (United States) (2014)
46. N.A. Cinel, S. Bütün, E. Özbay, Electron beam lithography designed silver nano-disks used as label free nano-biosensors based on localized surface plasmon resonance. *Opt. Express* **20**(3), 2587–2597 (2012)
47. Z. Yong, S. Zhang, C. Gong, S. He, Narrow band perfect absorber for maximum localized magnetic and electric field enhancement and sensing applications. *Sci. Rep.* **6**(1), 1–7 (2016)
48. L.L. Cong, X.Y. Cao, T. Song, J. Gao, J.X. Lan, Angular-and polarization-insensitive ultrathin double-layered metamaterial absorber for ultra-wideband application. *Sci. Rep.* **8**(1), 1–12 (2018)
49. A.H.A. Nohoji, M. Danaie, Highly sensitive refractive index sensor based on photonic crystal ring resonators nested in a Mach-Zehnder interferometer. *Opt. Quant. Electron.* **54**(9), 574 (2022)
50. Q. Duan, Y. Liu, S. Chang, H. Chen, J.H. Chen, Surface plasmonic sensors: sensing mechanism and recent applications. *Sensors* **21**(16), 5262 (2021)
51. L. Lin, Y. Zheng, Optimizing plasmonic nanoantennas via coordinated multiple coupling. *Sci. Rep.* **5**(1), 14788 (2015)
52. Y.E. Monfared, M. Qasymeh, Graphene-assisted infrared plasmonic metamaterial absorber for gas detection. *Results Phys.* **23**, 103986 (2021)
53. Z. Li, X. Sun, C. Ma, J. Li, X. Li, B.O. Guan, K. Chen, Ultranarrow-band metamaterial perfect absorber based on surface lattice resonance in a WS₂ nanodisk array. *Opt. Express* **29**(17), 27084–27091 (2021)
54. Q. Li, H. Tang, Y. Zhao, H. Liu, Z. Shen, T. Wang, J. Gao, Investigation of perfect narrow-band absorber in silicon nano hole array. *Opt. Express* **31**(19), 31644–31653 (2023)
55. X. Lu, L. Zhang, T. Zhang, Nanoslit-microcavity-based narrow band absorber for sensing applications. *Opt. Express* **23**(16), 20715–20720 (2015)
56. C.S. Park, S.S. Lee, Narrowband and flexible perfect absorber based on a thin-film nano-resonator incorporating a dielectric overlay. *Sci. Rep.* **10**(1), 17727 (2020)
57. Q. Li, Z. Li, X. Xiang, T. Wang, H. Yang, X. Wang, J. Gao, Tunable perfect narrow-band absorber based on a metal-dielectric-metal structure. *Coatings* **9**(6), 393 (2019)
58. X. He, J. Jie, J. Yang, Y. Han, S. Zhang, A mid-infrared narrow-band absorber based on a subwavelength fine-structured silicon-gold metagrating. *Appl. Sci.* **9**(23), 5022 (2019)
59. W. Ali, S. Iqbal, M. Ullah, X. Wang, An ultrahigh narrowband absorber close to the information communication window. *Plasmonics* **1–7** (2022)
60. X. Gu, R. Bai, X.R. Jin, Y.Q. Zhang, S. Zhang, Y. Lee, Ultranarrow-band perfect absorber based on high-order plasmonic resonance in metamaterial. *J. Nonlinear Opt. Phys. Mater.* **25**(01), 1650011 (2016)

Publisher's Note Springer Nature remains neutral with regard to jurisdictional claims in published maps and institutional affiliations.

Springer Nature or its licensor (e.g. a society or other partner) holds exclusive rights to this article under a publishing agreement with the author(s) or other rightsholder(s); author self-archiving of the accepted manuscript version of this article is solely governed by the terms of such publishing agreement and applicable law.